UKF-based Identification of Time-Varying Manual Control Behaviour

Rojer, Jim; Pool, Daan M.; Van Paassen, Marinus M.; Mulder, Max

DOI
10.1016/j.ifacol.2019.12.120

Publication date
2019

Document Version
Final published version

Published in
IFAC-PapersOnline

Available online at www.sciencedirect.com

ScienceDirect

IFAC Papers Online CONFERENCE PAPER ARCHIVE

IFAC PapersOnLine 52-19 (2019) 109–114

UKF-based Identification of Time-Varying Manual Control Behaviour

Jim Rojer, Daan M. Pool,[1] Marinus M. van Paassen, and Max Mulder

Control and Simulation, Faculty of Aerospace Engineering, TU Delft, 2629 HS, Delft, The Netherlands

Abstract: This paper describes a novel method for time-varying identification of Human Controller (HC) manual control parameters (called UKF-FPV), based on a steady-state (constant state covariance) Unscented Kalman Filter (UKF). This approach requires no *a priori* assumptions on the shape of HC parameter variations, which is a potential advantage over state-of-the-art methods such as the recently proposed MLE-APV approach, for which a sigmoid-shaped parameter variation is assumed. For a scenario where an HC performs a single-loop compensatory tracking task with time-varying controlled system dynamics, both identification methods are compared using Monte Carlo simulations and human-in-the-loop experiment data. Despite some lag in the HC parameter traces of UKF-FPV, the identification results and the HC model quality-of-fit obtained with both methods were found to match well for both the simulation and experiment data. For the experiment data, UKF-FPV even revealed clear "local" changes in HC parameters not captured by the MLE-APV approach, which confirms that HCs adapt *unpredictably* even in what are considered time-invariant conditions. Overall, the results show that an identification method that requires no *a priori* assumptions on HC parameter variations is of critical importance for a complete analysis of time-varying HC behaviour.

Keywords: Cybernetics, manual control, time-varying identification, Unscented Kalman Filter

1. INTRODUCTION

Despite major advances in automation and automatic control systems, Human Controllers (HCs) are still superior in their ability to adapt to changing external factors. Most of our current knowledge of human manual control behavior is restricted to *time-invariant* control tasks and control behavior (McRuer and Jex, 1967). Working towards a better understanding of HCs' unique capacity for adaptation (Young, 1969) – as well as its limitations – requires better, explicitly *time-varying* methods for the quantitative measurement and analysis of HC control behavior (Mulder et al., 2018). Furthermore, accurate identification and quantification of time-varying HC adaptation *in real time* would allow for improved performance monitoring systems and adaptive, personalized human-machine interfaces (Abbink et al., 2012; Mulder et al., 2018).

Over the years, several methods for time-varying identification of human control behavior have been proposed and tested, such as those based on Kalman filters (Schiess and Roland, 1975; Boer and Kenyon, 1998; Popovici et al., 2017), wavelets (Thompson et al., 2001; Zaal and Sweet, 2011), recursive ARX models (Van Grootheest et al., 2018; Plaetinck et al., 2018), and traditional HC model estimation over a sliding window (Zaal and Sweet, 2011) or with an *a priori* assumed model for the HC time variations included (Zaal, 2016). Despite these efforts, as recently summarized by Mulder et al. (2018), we currently still lack time-varying HC identification methods that: i) are sufficiently robust to the very high levels of human remnant and the variability inherent to HC data (McRuer and Jex, 1967), and (ii) do not make any *a priori* assumptions on the time-variation in the HC, assumptions which could cause other (types of) adaptations to be missed.

In this paper, a novel approach that uses a steady-state Unscented Kalman Filter (UKF) to estimate time-varying HC parameters, without any *a priori* assumptions on the shape of this variation, is developed. It is referred to as the "UKF with Free Parameter Variation" (UKF-FPV), and is tested on a time-varying HC scenario where HCs are forced to adapt to an induced change in the controlled element (CE) dynamics, matching an earlier experiment (Zaal, 2016). The results obtained are compared to those of the state-of-the-art method of (Zaal, 2016), here referred to as "Maximum Likelihood Estimation with Assumed Parameter Variation" (MLE-APV), which estimates HC adaptation using an assumed model for the parameter adjustments. We present a comparison of the HC identification results obtained with both methods on both Monte Carlo simulation data, as well as experiment data from a dedicated human-in-the-loop experiment.

2. HUMAN CONTROLLER IDENTIFICATION

2.1 Control Task

We consider the identification of time-varying HC behavior in a single-loop compensatory tracking task, see Fig. 1, matching earlier investigations (Zaal, 2016; Van Grootheest

[1] Corresponding author: d.m.pool@tudelft.nl

10.1016/j.ifacol.2019.12.120

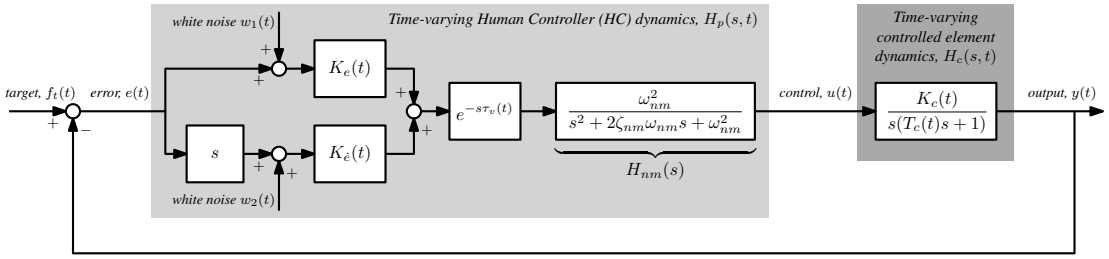

Fig. 1. Block diagram of the time-varying single-loop compensatory tracking task.

et al., 2018; Plaetinck et al., 2018). Here, a human controller gives inputs u to the controlled element $H_c(s,t)$ to continuously minimize the tracking error signal e. It is well-known that in such tasks HCs systematically adapt their control dynamics $H_p(s,t)$ to changes in task variables (McRuer and Jex, 1967; Young, 1969).

This paper focuses on a tracking task matching the pitch task performed in the experiment of Zaal (2016). A deliberate instantaneous change in the controlled dynamics $H_c(s,t)$ (see Fig. 1) is induced, i.e., from an initial setting that approximates a K/s system (H_{c_1}) to a final setting that approximates a K/s^2 system (H_{c_2}):

$$H_{c_1}(s) = \frac{90}{s^2+6s} \quad \Rightarrow \quad H_{c_2}(s) = \frac{30}{s^2+0.2s} \tag{1}$$

The change in $H_c(s,t)$ is induced by varying the gain $K_c(t)$ and lag time-constant $T_c(t)$ of the controlled system over time using a sigmoid function, as defined for $K_c(t)$:

$$K_c(t) = K_{c_1} + \frac{K_{c_2} - K_{c_1}}{1+e^{-G(t-M)}} \tag{2}$$

Here, K_{c_1} and K_{c_2} indicate the initial and final asymptotic settings for $K_c(t)$. The M and G parameters – the sigmoid's central time and abruptness parameters, respectively – are set to 50 s and 100 s^{-1}, for a 90-second tracking run length, matching (Zaal, 2016).

2.2 Human Control Model

As shown in Fig. 1, for modeling time-varying HC behavior in tracking tasks we use a traditional quasi-linear HC model as proposed by McRuer and Jex (1967), but with time-varying model parameters. Fig. 1 shows HC control dynamics $H_p(s,t)$ composed of proportional-derivative equalization term parameterized with two gains (K_e and $K_{\dot{e}}$), an HC time delay τ_v, and a second-order neuromuscular system model $H_{nm}(s)$ with natural frequency (ω_{nm}) and damping ratio (ζ_{nm}) parameters. Note that the HC model shown in Fig. 1 is mathematically equivalent to the models proposed in (McRuer and Jex, 1967) with an operator gain and lead time-constant.

For the considered task, it is known that HCs will need to adapt from performing mostly proportional control (high K_e, low $K_{\dot{e}}$) for H_{c_1} to performing significant lead equalization (reduced K_e, high $K_{\dot{e}}$) for H_{c_2} (Zaal, 2016). The other HC parameters, especially those of neuromuscular dynamics (i.e., ω_{nm} and ζ_{nm}) have been found to hardly vary due to a time-varying change in $H_c(s,t)$ (Zaal, 2016).

Finally, Fig. 1 shows that to complete the quasi-linear operator model, an implementation of the remnant model of (Levison et al., 1969) is included. This model accounts for HC remnant that arises from observation errors, as well as execution errors in both K_e and $K_{\dot{e}}$, with two independent white noise inputs – w_1 and w_2 in Fig. 1 – on the error and error rate responses. As Levison et al. (1969) found that the power of both noise inputs scales with their respective total signal variance, according to $\sigma_{w_1}^2/\sigma_e^2 = \sigma_{w_2}^2/\sigma_{\dot{e}}^2 = c$, the noise fraction coefficient c is the only free parameter of this model.

2.3 Time-Varying Human Operator Identification

MLE with Assumed Parameter Variation (MLE-APV) We will compare two different time-varying HC identification techniques. The first is developed by Zaal (2016), and uses an output-error method with a Maximum-Likelihood (ML) cost function *on the complete time-varying tracking data series* to fit an HC model as shown in Fig. 1. In this approach the HC equalization parameters are assumed to vary according to sigmoids, as given in Eq. (2), with the same M and G values for all parameters. Hence, in this paper, this approach is referred to as "Maximum Likelihood Estimation with Assumed Parameter Variation" (MLE-APV). The resulting total parameter vector for this approach is thus given by:

$$\Theta_{\text{MLE-APV}} = [K_{e_1}\ K_{e_2}\ K_{\dot{e}_1}\ K_{\dot{e}_2}\ M\ G\ \tau_v\ \zeta_{nm}\ \omega_{nm}]^T \tag{3}$$

As proposed by Zaal (2016), this optimization problem is solved by subsequent application of a genetic algorithm (to obtain a rough estimate of $\Theta_{\text{MLE-APV}}$ close to the global optimum) and a linear unconstrained Gauss-Newton optimization (to converge to the optimum). Note that with this approach the full measured time traces of time-varying HC behavior result in *a single* estimate of $\Theta_{\text{MLE-APV}}$.

UKF with Free Parameter Variation (UKF-FPV) The second time-varying identification approach considered is based on an Unscented Kalman Filter (UKF) estimator. Given that no HC adaptation is expected for the considered scenario, the HC neuromuscular parameters (ω_{nm} and ζ_{nm}) are assumed to be time-invariant and known *a priori*. The three remaining HC model parameters – K_e, $K_{\dot{e}}$, and τ_v – are estimated *at each time step* as the current most likely value of these parameters to explain the measured data, with no prior assumptions. For this second approach, here referred to as "UKF with Free Parameter Variation" (UKF-FPV), the following parameter vector is thus estimated *at each time step*:

$$\Theta = [K_e\ K_{\dot{e}}\ \tau_v]^T \tag{4}$$

For the UKF-FPV approach, the system model implemented the HC model shown in Fig. 1, with the error signal

e and the control signal u as the system input and output signals, respectively. The state vector of the system model was chosen to only consist of the estimated HC model parameters, while the output equation implemented the HC model – using a fifth order Padé approximation for including the HC delay term – in the nonlinear output function h. The resulting UKF state and measurement equations, in discrete notation, are given by:

$$\Theta_k = \Theta_{k-1} + w_k \tag{5}$$

$$u_k = h(\Theta_k, e_k) + v_k \tag{6}$$

In Eq. (5), Θ is the parameter vector given by Eq. (4) and w_k is the system noise vector. In Eq. (6), u_k and e_k are the k^{th} samples of the HC output and input, respectively, and v_k is the observation noise vector. Eq. (5) shows that the parameters were modeled as a "random walk", which explicitly shows that no model was assumed for parameter variation over time. Instead, the parameter vector Θ_k is estimated recursively from the relative magnitude of the state and measurement covariances.

As the HC model implemented in the output function h is nonlinear in its parameters – e.g., due to the included Padé delay model – a nonlinear KF is required. In this paper, we propose to use the UKF for convenience, as the UKF uses repeated point evaluations (sigma points) to estimate the nonlinear distribution properties, instead of relying on cumbersome linearization of the nonlinear system model.

We used a UKF implementation based on Van der Merwe (2004), with additive noise terms. For the current application of the UKF to estimate time-varying HC parameters, a number of key implementation and configuration choices were made, driven by the authors' understanding of the physical interpretation of the UKF and experience:

- *UKF sigma point settings*: As explained by Julier and Uhlmann (2004), the α, β and κ parameters control the sigma point distribution and hence the accuracy and numerical stability of the UKF. Here, typical values for all parameters based on (Julier and Uhlmann, 2004) were used, see Table 1, which ensured suppression of errors due to high-order Taylor expansion terms ($\alpha = 10^{-3}$, $\kappa = 3$) for assumed Gaussian estimation errors ($\beta = 2$).
- *Measurement correction iterations:* To accurately estimate HC delays, it was found to be required to iterate the observation equation over a past window at UKF each time step. This is expected, as parameter variations that affect the HC lags cannot be estimated over a single time step, as their effects are intrinsically linked to earlier inputs. Here a past window of 0.75 seconds was used, a value that was heuristically tuned and found to make the UKF sufficiently robust to even the highest encountered HC delays.
- *System noise/parameter covariance:* Critical to the performance of any Kalman filter is the tuning of the system and observation noise stochastic properties through the associated covariance matrices. For a random walk model as given by Eq. (5), the system noise covariance (i.e., "Q" corresponding to w_k) loses its physical interpretation and is generally tuned to optimize estimation performance. Hence, here it is chosen to forego tuning of the system noise covariance matrix (Q) in favor of directly selecting a steady-state, and diagonal, state covariance matrix (P).

  Table 1 lists the final settings used for the steady-state covariances corresponding to each estimated parameter in Θ, i.e., $\sigma^2_{K_e}$, $\sigma^2_{K_{\dot{e}}}$, and $\sigma^2_{\tau_v}$. These values were determined from extensive heuristic tuning a set of simulated HC data, for which these settings were found to provide reliable and representative estimation results *independent* of the remnant noise power. It should be noted that an "optimal" tuning does not exist: through the state covariance matrix we now directly control the trade-off between smoothing and tracking speed of the parameter estimates.
- *Measurement noise covariance:* In the considered scenario, HCs significantly adapt their control dynamics $H_p(s,t)$, which also results in increased remnant noise after the transition in $H_c(s,t)$ (Van Grootheest et al., 2018). This increase in remnant is also modeled in Fig. 1 with the Levison et al. (1969) remnant model. Hence, for the UKF the same remnant model is also implemented to achieve an "adaptive" measurement covariance ("R"), here a scalar due to our single model output, see Table 1. The update equation for R is easily derived given that w_1 and w_2 are independent. An overall noise level scaling coefficient c_R was needed to achieve equivalent estimation performance for different remnant noise levels, see Table 1.

Table 1. Steady-state UKF settings.

Parameter	Value	Unit
α	10^{-3}	[-]
β	2	[-]
κ	3	[-]
$\sigma^2_{K_e}$	$3.5 \cdot 10^{-5}$	[-]
$\sigma^2_{K_{\dot{e}}}$	$3.5 \cdot 10^{-5}$	[s^2]
$\sigma^2_{\tau_v}$	$3.5 \cdot 10^{-5}$	[s^2]
R	$c_R\left(\sigma^2_e(t)K^2_e(t) + \sigma^2_{\dot{e}}(t)K^2_{\dot{e}}(t)\right)$	[deg^2]
c_R	$\sigma^2_n/\sigma^2_u = 0.05 \longrightarrow 0.5$	[-]
	$\sigma^2_n/\sigma^2_u = 0.15 \longrightarrow 1.5$	[-]
	$\sigma^2_n/\sigma^2_u = 0.25 \longrightarrow 2.5$	[-]

3. TWO DATA SETS

The two time-varying HC identification techniques introduced above were tested on human-in-the-loop experiment and Monte Carlo simulation data of the same control task. This section provides all relevant details of how we obtained the experimental and simulation data.

3.1 Experiment Data

The human-in-the-loop experiment was mostly matched to the earlier experiment of Zaal (2016), to enhance comparability. While also data for other time-varying scenarios were collected, this paper will focus on data from the condition where a single-loop pitch attitude tracking task (see Fig. 1) was performed with $H_c(s,t)$ varying from H_{c_1} to H_{c_2} with a step-like change, i.e., with $G = 100$ s^{-1} and $M = 50$ s as the sigmoid parameters for Eq. (2).

The experiment was performed in TU Delft's Human-Machine Interaction Laboratory (HMILab), see Fig. 2,

where a electro-hydraulic sidestick was used for giving control inputs. Participants gave fore-aft stick inputs to perform the pitch tracking task, for which the tracking error was shown as the vertical displacement of the "target" line on the simplified flight display shown in Fig. 2.

Fig. 2. Human-in-the-loop experiment setup.

Data were collected from six participants, all students and staff of TU Delft. All participants were right-handed males, with an average age of 27.7 years. Before the start of the experiment, the participants received a briefing and provided written informed consent. Participants were first trained by performing a number of tracking runs until their performance stabilized. Then, six more measurement runs were performed to collect the experiment data.

3.2 Simulation Data

To generate the simulation data, simulations of the closed-loop control task of Fig. 1 were performed in Matlab. The task parameters (i.e., f_t, $H_c(s,t)$, etc.) were identical to those tested in the experiment. The simulated time-varying HC dynamics $H_p(s,t)$ were based on the average measured human controller behavior reported by Zaal (2016). The neuromuscular parameters, ω_{nm} and ζ_{nm}, were kept constant at values of 11.25 rad/s and 0.35, respectively. The other three HC parameters – K_e, $K_{\dot{e}}$, and τ_v – were varied over time using a sigmoid function as defined in Eq. (2). The initial and final parameter settings used for all parameters are listed in Table 2. The sigmoid rate of change was the same for all parameters, i.e., $G = 2$ s^{-1} based on Zaal (2016)'s results, but the sigmoid central time M was deliberately varied, to induce a mismatch with the assumed parameter variation for MLE-APV. Furthermore, three additional "perturbations" – of the form $Ae^{G(t-M)^2}$ with $A = 0.01$, $G = -5$, -1, and -1, and $M = 51$ s, 55 s, and 57 s, respectively – were added to the simulated variation in $K_{\dot{e}}$.

Table 2. Settings for simulated $H_p(s,t)$.

Parameter	Initial value	Final value	M [s]	G [s^{-1}]
K_e	0.09	0.07	52	
$K_{\dot{e}}$	0.036	0.084	53	2
τ_v	0.28	0.25	57	

For this scenario, Monte Carlo simulations were performed with 100 different realizations of the remnant noise inputs w_1 and w_2, see Fig. 1. Furthermore, for quantitative insight into the effect of the remnant noise on the obtained results, the remnant noise intensity was varied over three different levels of the total noise contribution to the simulated control signal, i.e., $\sigma_n^2/\sigma_u^2 = 0.05$, 0.15, 0.25. This was achieved by setting the c parameter of the Levison et al. (1969) remnant model to 0.25, 0.5, and 0.75, respectively, for band-limited (40 rad/s) white noise signals.

4. RESULTS

4.1 Identified HC Parameter Variations

Fig. 3 shows parameter estimates results obtained with both the MLE-APV and UKF-FPV approaches detailed in Section 2.3. The simulation results for the three considered remnant levels – i.e., $\sigma_n^2/\sigma_u^2 = 0.05$, 0.15, and 0.25 – are shown in Fig. 3(a) to (c). Fig. 3(d) shows the experiment data results, with two examples that were taken from the full experiment dataset: one shows a "slow' HC parameter adjustment, while the other represents a 'fast' HC adaptation. These two examples were selected to illustrate the capabilities of the two identification methods.

For the simulation data (Fig. 3(a) to (c)), the true HC parameter variations are indicated in red, while the MLE and UKF results (mean and 2σ bounds over 100 noise realizations) are presented in black and blue, respectively. With increasing remnant we observe, as expected, increasingly slower convergence for the UKF after the parameter variations occur. With higher σ_n^2/σ_u^2, more data points are needed to successfully discriminate between remnant and parameter variation. This limited tracking speed means that the UKF is unable to follow the additional perturbation on $K_{\dot{e}}$ for any σ_n^2/σ_u^2. Due to the use of the full time traces and the matching shape of the HC adaptation, the MLE method consistently retrieves the applied HC parameter variations, especially for $K_{\dot{e}}$. The MLE method, as expected, also does not capture the perturbations applied to $K_{\dot{e}}$. For K_e the correct initial and final values are estimated by MLE, but around the change in $H_c(s,t)$ the results are clearly not as accurate. Finally, the MLE approach assumes a constant estimated delay, but as can be verified from Fig. 3 this incorrect assumption does not affect the other parameter estimates. The UKF is seen to estimate the correct trend in τ_v, but cannot track the quickness of the variation.

For the experiment data in Fig. 3(d), the MLE and UKF results are presented for two example runs. To avoid graph clutter, the data for example 2 are presented with a +0.05 offset for all parameters. Fig. 3(d) shows that both methods estimate matching parameter values and time-variations for both datasets. As expected for a recursive method, the UKF lags behind the estimated MLE parameter variation. On the other hand, the UKF data show evidence of multiple "local" HC adaptations during intervals where $H_c(s,t)$ was in fact constant. For the 'example 1' data such an instance occurs between between 20-40 sec, where this participant showed a consistent temporary increase in K_e. Similarly, the 'example 2' data show a locally reduced $K_{\dot{e}}$ between 35-50 sec compared to the MLE result. Such instances show that, as expected (Mulder et al., 2018), real HCs adapt continuously, and not always predictably, in time-invariant conditions.

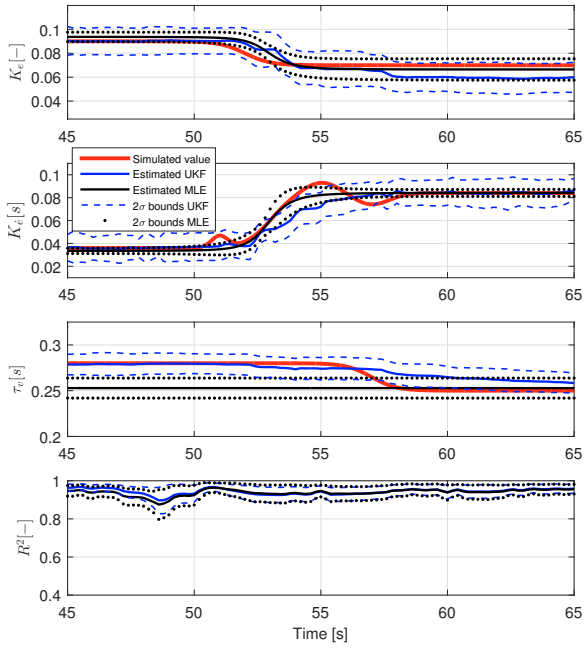

(a) Simulation, $\sigma_n^2/\sigma_u^2 = 0.05$

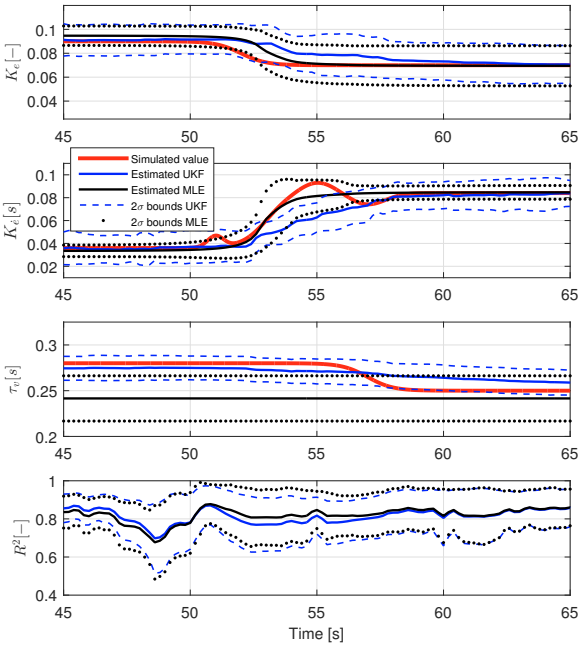

(b) Simulation, $\sigma_n^2/\sigma_u^2 = 0.15$

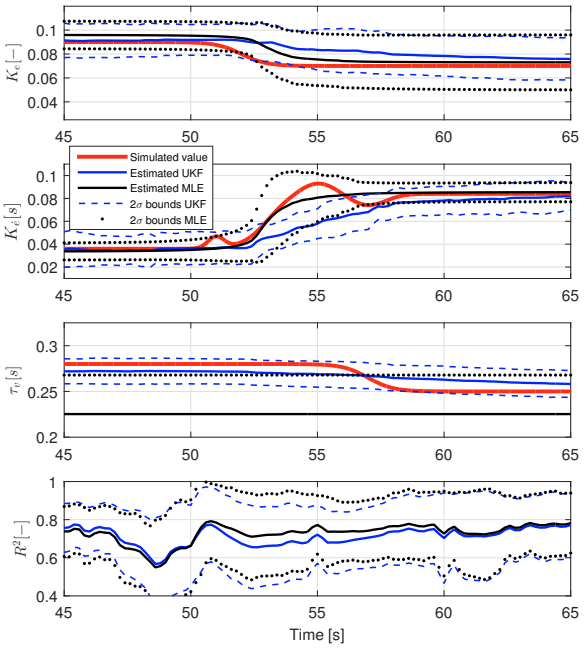

(c) Simulation, $\sigma_n^2/\sigma_u^2 = 0.25$

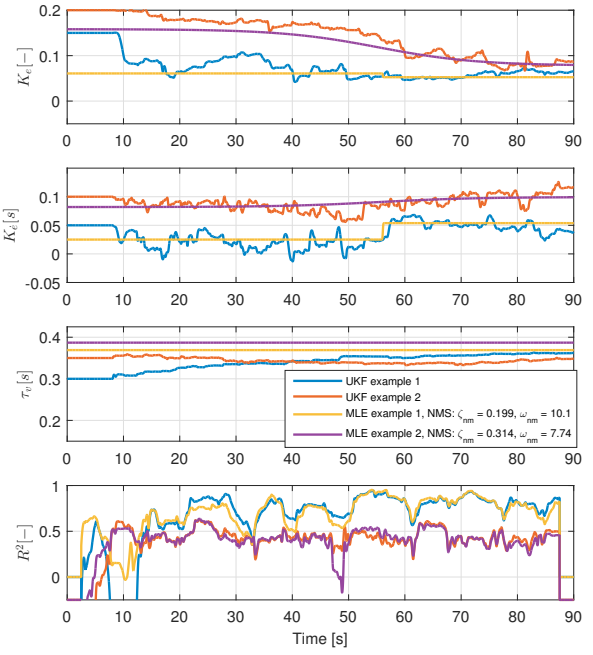

(d) Experiment data

Fig. 3. Monte Carlo simulation parameter estimates for $\sigma_n^2/\sigma_u^2 = 0.05$, 0.15, and 0.25 (100 remnant realizations) and example experiment data results for two representative runs.

4.2 HC Identification Quality-of-Fit

In addition to the HC parameter traces for both methods, Fig. 3 also provides a quantitative comparison of the quality-of-fit achieved with both the MLE-APV and UKF-FPV methods. Hereto, the bottom-most graphs in all subfigures show the corresponding traces of the coefficient-of-determination R^2 of both methods. As also done for the parameter results, a -0.25 offset is applied to the R^2 for 'example 2' to avoid clutter. These R^2-traces were calculated at each time instant over a 5-second centered window. Overall, the R^2 data show that the overall quality-of-fit attained for both methods is comparable and at the level expected for modeling of HC behavior based on single tracking run data, i.e., $0.6 - 1.0$ (Van Grootheest et al., 2018). For the simulation data in Fig. 3(a) to (c) it can be seen that R^2 consistently decreases with increasing σ_n^2/σ_u^2, as expected for increased noise on the data. Furthermore, the R^2-traces also show that the UKF's increasingly slow tracking of the HC parameter changes with increasing remnant noise result in consistently degraded quality-of-fit after the transition compared to MLE. For the experiment data, significant local drops in R^2 are observed for the MLE estimates during the instances where the UKF data suggest local HC adaptations not captured by MLE, i.e., around 48 seconds for 'example 2' data.

Overall, our UKF data in Fig. 3 thus provide evidence to support the validity of the MLE-APV approach as proposed by Zaal (2016) for this time-varying HC adaptation scenario. While the results of an approach such as MLE-APV thus capture the "global" and dominant HC parameter variations as expected in response to a time-varying change in $H_c(s,t)$, our UKF data also indicate that smaller local HC parameter adjustments are not detected. Such variations in HC control behavior can only be identified with a recursive estimation method that requires no *a priori* assumptions on the occurring HC parameter variations, which our novel UKF-FPV approach provides.

5. CONCLUSIONS

This paper presents a novel time-varying human controller parameter estimation approach, based on a steady-state (constant state covariance) Unscented Kalman Filter (UKF). By explicitly modelling all estimated HC model parameters as a random walk, our proposed UKF-FPV approach can estimate time-variations in these parameters from measured HC data without making any *a priori* assumptions on the nature and time occurrence of these HC adaptations. The time-varying HC identification results obtained with UKF-FPV are compared to those of the state-of-the-art MLE-APV method, for which an *a priori* assumed model for HC parameter adjustments is included. Overall, the identified time traces of HC parameters, as well as the HC model quality-of-fit, obtained with both methods were found to match well for both simulation and experiment datasets. With the matching outcomes for the experiment data, we were able to conclude with our UKF-FPV approach that the assumed parameter variation for MLE-APV is indeed suitable for the considered scenario. Furthermore, from the UKF-FPV results, HCs were found to show instances of local adaptation, also during intervals with constant conditions. This shows the importance of time-varying HC identification methods such as our UKF-FPV approach for performing a complete, and unbiased, analysis of the adapting human controller.

REFERENCES

Abbink, D.A., Mulder, M., and Boer, E.R. (2012). Haptic shared control: smoothly shifting control authority? *Cognition, Technology & Work*, 14(1), 19–28.

Boer, E.R. and Kenyon, R.V. (1998). Estimation of Time-Varying Delay Time in Nonstationary Linear Systems: An Approach to Monitor Human Operator Adaptation in Manual Tracking Tasks. *IEEE Trans. on Systems, Man and Cybernetics, Part A*, 28(1), 89–99.

Julier, S.J. and Uhlmann, J.K. (2004). Unscented Filtering and Nonlinear Estimation. *Proc. of the IEEE*, 92(3), 401–422.

Levison, W.H., Baron, S., and Kleinman, D.L. (1969). A Model for Human Controller Remnant. *IEEE Trans. on Man-Machine Systems*, 10(4), 101–108.

McRuer, D.T. and Jex, H.R. (1967). A Review of Quasi-Linear Pilot Models. *IEEE Trans. on Human Factors in Electronics*, HFE-8(3), 231–249.

Mulder, M., Pool, D.M., Abbink, D.A., Boer, E.R., Zaal, P.M.T., Drop, F.M., Van der El, K., and Van Paassen, M.M. (2018). Manual Control Cybernetics: State-of-the-Art and Current Trends. *IEEE Trans. on Human-Machine Systems*, 48(5), 468–485.

Plaetinck, W., Pool, D.M., Van Paassen, M.M., and Mulder, M. (2018). Online Identification of Pilot Adaptation to Sudden Degradations in Vehicle Stability. In *Proc. of the 2nd IFAC Conf. on Cyber-Physical & Human Systems, Miami (FL)*.

Popovici, A., Zaal, P.M.T., and Pool, D.M. (2017). Dual Extended Kalman Filter for the Identification of Time-Varying Human Manual Control Behavior. In *Proc. of the AIAA Modeling and Simulation Technologies Conference, Denver (CO)*, AIAA-2017-3666.

Schiess, J.R. and Roland, V.R. (1975). Kalman Filter Estimation of Human Pilot-Model Parameters. Technical Report NASA-TN-D-8024, NASA Langley Research Center, Hampton (VA).

Thompson, P.M., Klyde, D.H., and Brenner, M.J. (2001). Wavelet-Based Time-Varying Human Operator Models. In *Proc. of the AIAA Atmospheric Flight Mechanics Conference, Montreal (CA)*, AIAA-2001-4009.

Van der Merwe, R. (2004). *Sigma-Point Kalman Filters for Probabilistic Inference in Dynamic State-Space Models*. Ph.D. thesis, OGI School of Science & Engineering at Oregon Health & Science University.

Van Grootheest, A., Pool, D.M., Van Paassen, M.M., and Mulder, M. (2018). Identification of Time-Varying Manual Control Adaptations with Recursive ARX Models. In *Proc. of the AIAA Modeling and Simulation Technologies Conference, Kissimmee (FL)*, AIAA-2018-0118.

Young, L.R. (1969). On Adaptive Manual Control. *Ergonomics*, 12(4), 635–674.

Zaal, P.M.T. (2016). Manual Control Adaptation to Changing Vehicle Dynamics in Roll-Pitch Control Tasks. *J. of Guid., Contr., and Dyn.*, 39(5), 1046–1058.

Zaal, P.M.T. and Sweet, B.T. (2011). Estimation of Time-Varying Pilot Model Parameters. In *Proc. of the AIAA Modeling and Simulation Technologies Conference, Portland (OR)*, AIAA-2011-6474.